

# Sensitivity enhancement of nanoplasmonic sensors in low refractive index substrates

Björn Brian<sup>1</sup>, Borja Sepúlveda<sup>2,\*</sup>, Yury Alaverdyan<sup>3</sup>, Laura M. Lechuga<sup>2</sup>, Mikael Käll<sup>1</sup>

<sup>1</sup>Applied Physics  
Chalmers University of Technology  
SE-412 96 Göteborg, Sweden

<sup>2</sup>Nanobiosensors and Molecular Nanobiophysics Group  
Research Center on Nanoscience and Nanotechnology (CIN2) CSIC-ICN  
08193 Bellaterra, Barcelona, Spain

<sup>3</sup>Cavendish Laboratory, University of Cambridge, Cambridge CB3 0HE, United Kingdom

\*Corresponding author: [borja.sepulveda@cin2.es](mailto:borja.sepulveda@cin2.es)

**Abstract:** Metal films perforated by nanoholes constitute a powerful platform for surface plasmon resonance biosensing. We find that the refractive index sensitivity of nanohole arrays increases if their resonance is red-shifted by increasing the separation distance between holes. However, an additional sensitivity enhancement occurs if the nanohole sensors are manufactured on low index substrates, despite the fact such substrates significantly blue-shift the resonance. We find a ~40% higher bulk refractive index sensitivity for a system of ~100 nm holes in 20 nm gold films fabricated on Teflon substrates ( $n=1.32$ ) compared to the case when conventional glass substrates ( $n=1.52$ ) are used. A similar improvement is observed for the case when a thin layer of dielectric material is deposited on the samples. These results can be understood by considering the electric field distribution induced by the so-called antisymmetric surface plasmon polariton in the thin gold films.

© 2009 Optical Society of America

**OCIS codes:** (130.6010) Sensors; (240.6680) Surface Plasmons; (310.6845) Thin film devices and applications; (260.3910) Metal optics

## References and links

1. B. Liedberg, C. Nylander, and I. Lundström, "Surface plasmon resonance for gas detection and biosensing," *Sens. Act.* **4**, 299-304 (1983).
2. M. M. Miller and A. A. Lazarides, "Sensitivity of metal nanoparticle surface plasmon resonance to the dielectric environment," *J. Phys. Chem. B* **109**, 21556-21565 (2005).
3. R. Karlsson, "SPR for molecular interaction analysis: a review of emerging application areas," *J. Mol. Recognit.* **17**, 151-161 (2004).
4. A. J. Haes, W. P. Hall, L. Chang, W. L. Klein, and R. P. Van Duyne, "A localized surface plasmon resonance biosensor: First steps toward an assay for Alzheimer's disease," *Nano Lett.* **4**, 1029-1034 (2004).
5. K. Shafer-Peltier, C. Haynes, M. Glucksberg, and R. Van Duyne, "Toward a Glucose Biosensor Based on Surface-Enhanced Raman Scattering," *J. Am. Chem. Soc.* **125**, 588-593 (2003).
6. M. P. Kreuzer, R. Quidant, G. Badenes, and M. P. Marco, "Quantitative detection of doping substances by a localised surface plasmon sensor," *Biosens. Bioelectron.* **21**, 1345-1349 (2006).
7. K. Fujiwara, H. Watarai, H. Itoh, E. Nakahama, and N. Ogawa, "Measurement of antibody binding to protein immobilized on gold nanoparticles by localized surface plasmon spectroscopy," *Anal. Bioanal. Chem.* **386**, 639-644 (2006).
8. L. Olofsson, T. Rindzevicius, I. Pfeiffer, M. Käll, and F. Hook, "Surface-based gold-nanoparticle sensor for specific and quantitative DNA hybridization detection," *Langmuir* **19**, 10414-10419 (2003).
9. T. Rindzevicius, Y. Alaverdyan, B. Sepúlveda, T. Pakizeh, M. Käll, R. Hillenbrand, J. Aizpurua, and F. J. Garcia de Abajo, "Nanohole plasmons in optically thin gold films," *J. Phys. Chem. C* **111**, 1207-1212 (2007).
10. B. Sepúlveda, Y. Alaverdyan, J. Alegret, M. Käll, and P. Johansson, "Shape effects in the localized surface plasmon resonance of single nanoholes in thin metal films," *Opt. Express* **16**, 5609-5616 (2008).
11. Y. Alaverdyan, B. Sepúlveda, L. Eurenium, E. Olsson, and M. Käll, "Optical antennas based on coupled nanoholes in thin metal films," *Nature Phys.* **3**, 884-889 (2007).
12. T. Rindzevicius, Y. Alaverdyan, A. Dahlin, F. Höök, D. S. Sutherland, and M. Käll, "Plasmonic sensing characteristics of single nanometric holes," *Nano Lett.* **5**, 2335-2339 (2005).

13. A. Dahlin, M. Zach, T. Rindzevicius, M. Käll, D. S. Sutherland, and F. Höök, "Localized surface plasmon resonance sensing of lipid-membrane-mediated biorecognition events," *J. Am. Chem. Soc.* **127**, 5043-5048 (2005).
  14. P. Hanarp, M. Kall, and D. S. Sutherland, "Optical properties of short range ordered arrays of nanometer gold disks prepared by colloidal lithography," *J. Phys. Chem. B* **107**, 5768-5772 (2003).
  15. S. Link and M. A. El-Sayed, "Spectral properties and relaxation dynamics of surface plasmon electronic oscillations in gold and silver nanodots and nanorods," *J. Phys. Chem. B* **103**, 8410-8426 (1999).
  16. H. Wang, D. W. Brandl, L. Fei, P. Nordlander, and N. J. Halas, "Nanorice: A Hybrid Plasmonic Nanostructure," *Nano Lett.* **6**, 827-832 (2006).
  17. E. Larsson, J. Alegret, M. Mikael Käll, and D. S. Sutherland, "Sensing characteristics of NIR localized surface plasmon resonances in gold nanorings for application as ultrasensitive biosensors," *Nano Lett.* **7**, 1256-1263 (2007).
  18. P. Hanarp, *Optical properties of nanometer disks, holes and rings prepared by colloidal lithography* (Chalmers University of Technology, Göteborg, 2003).
  19. B. Sepulveda, L. Lechuga, and G. Armelles, "Magneto-optic effects in surface-plasmon-polaritons slab waveguides," *J. Lightwave Technology*, **24**, 945-955 (2006).
  20. L. S. Jung, C. T. Campbell, T. M. Chinowsky, M. N. Mar, and S. S. Yee, "Quantitative Interpretation of the Response of Surface Plasmon Resonance Sensors to Adsorbed Films," *Langmuir* **14**, 5636-5648 (1998).
  21. T. Rindzevicius, Y. Alaverdyan, M. Kall, W. A. Murray, and W. L. Barnes, "Long-Range Refractive Index Sensing Using Plasmonic Nanostructures," *J. Phys. Chem. C* **111**, 11806-11810 (2007).
- 

## 1. Introduction

The intense and confined electromagnetic fields generated by surface plasmons in metal films and nanostructures have been used for label free biosensing since 1983[1]. In the case of metal nanostructures, the surface plasmon resonance (SPR) can be detected as a peak in the optical scattering, reflection or extinction spectra. The spectral position of the resonance is highly dependent on the shape, distribution and electrodynamic environment of the nanostructures. In particular, the strong dependence of the SPR on the permittivity of the surrounding medium constitutes the sensing principle of metal nanostructures. Thus, a local increase in the refractive index in the close proximity of the nanostructure, as the one induced by adsorbed biomolecules, produces a red-shift of the resonance position [2].

There are several advantages associated with nanoplasmonic sensing compared to conventional surface plasmon polariton (SPP) sensors employing thin metal films. Advantages include a much higher degree of miniaturization, restricted only by the diffraction limit of the read-out optics. This enables an unprecedented potential for high density multiplexing. In addition, light can induce plasmons in the metal nanostructures directly, without the requirement of other optical coupling elements. Consequently, this technology is very promising due to an ever-increasing demand for high-throughput screening applications, as for example, for the discovery of new drug candidates [3].

Biosensors based on metal nanoparticles fabricated with nanosphere lithography on a solid support have been successfully employed in the detection of ADDL (amyloid-derived diffusible ligands) oligomers, found in elevated concentrations in the brain tissue of Alzheimer's disease patients[4]. These nanostructures have also been proposed for the detection of glucose in diabetes patients [5]. Colloidal gold nanoparticles have been used as transducer elements in the detection of doping substances [6], different proteins [7] or DNA hybridization [8].

Other attractive metal nanostructures for biosensing applications are nanoholes in optically thin metal layers. Unlike nanoparticles, these nanostructures combine the properties of SPPs in thin metal layers with the localized surface plasmon resonance (LSPR) created by the nanoholes [9]. This combination arises by the induced electric dipole excited by the incident light in the nanoholes, which acts as a source of antisymmetric SPPs in the thin metal film. Such SPPs interact with the nearest nanoholes modifying their net dipole moment and, therefore, drastically changing their radiation properties. Nanoholes in thin films present several optical features making them interesting for sensing applications as, for example: i) the significant increase in the amplitude of the electric dipole moment and red-shift of the resonance when the polarization of the incoming light is parallel to the short axis of elongated nanoholes [10]; ii) large amplification of the scattering intensity and spectral narrowing of the

resonance when the distances between nanoholes are tuned to half the wavelength of the antisymmetric SPP [11]; iii) wide tunability of the resonance position of the nanohole assembly that can be achieved by simply changing the separation distance between nanoholes [11].

In addition, these nanohole systems feature an interesting chemical contrast between the metal surface and the exposed substrate at the bottom of the nanoholes. The chemical difference of the surface has been used to selectively adsorb biotin-BSA on the metal film [12]. The chemical contrast has also been used to induce the rupture of phospholipid vesicles in the bottom of the nanoholes, forming supported phospholipid bilayers [13]. The attractive optical properties together with the chemical contrast are undisputedly interesting to develop for the investigation of membrane proteins which are essential in the communication between the extracellular and intracellular domains, and for their application as drug targets. To add even more interest, short-range ordered nanoholes in thin metal films can be inexpensively fabricated with colloidal lithography techniques over large area [14].

The sensing principle of nanoplasmonic systems is based on the shift of the resonance position of the nanostructures when the refractive index of the surrounding environment changes. Consequently, their sensitivity to the changes of the refractive index can be defined as:

$$\eta_{bulk} = \frac{\delta\lambda_{SPR}}{\delta n_d} \quad (1)$$

where  $\lambda_{SPR}$  represents the wavelength position of the resonance and  $n_d$  is the refractive index of the surrounding dielectric. It has been shown that the sensitivity of the plasmonic nanoparticle systems increases as the peak position of the resonance is tuned to near infrared spectral region (NIR) [2]. Therefore, many different nanostructures have been proposed and fabricated to shift the LSPR peak position to NIR, such as nanorods [15], core-shell nanoparticles [16] and nanorings [17]. However, in many sensing applications, only a fraction of the electromagnetic field around the nanostructures is employed. For these applications, a surface sensitivity, defined as:

$$\eta_{surface} = \frac{\delta\lambda_{SPR}}{\delta d_b} \quad (2)$$

where  $d_b$  is the thickness of the adsorbed biological layer, will give a more accurate description of the sensitivity to the local changes in the surface refractive index caused by the biochemical interactions.

In this paper, we present the strong impact that the substrate has on the bulk and surface sensitivities of nanohole biosensing systems. We show that the reduction of the refractive index of the substrate induces a very significant increase in the bulk and surface sensitivities. This improvement is achieved despite the fact that the peak position of the resonance is blue-shifted when the substrate refractive index is reduced. This effect is due to the change of the electromagnetic field distribution in the nanoholes arrays, which, in low index substrates, is concentrated in the sensing region.

The paper is organized as follows: first, the bulk sensitivity as a function of the peak position was studied using ordered arrays of nanoholes prepared by focused ion beam (FIB) milling. This was done to enable a just comparison of the different substrates since the dielectric environment on both sides of the perforated gold film affects the peak position. Second, since colloidal lithography is often applied when preparing sensor surfaces, this technique was used in the fabrication of short-range ordered hole arrays on different substrates.

## 2. Fabrication and optical characterization

Nanohole samples were fabricated using different techniques. Ordered nanohole chains were fabricated using focused ion beam (FIB) etching. In short, a 1 nm Ti adhesion layer and a 20

nm thick gold film were thermally evaporated on a glass substrate. Subsequently, eight evenly separated nanoholes were created using FIB (FEI Strata 235 Dual Beam) milling.

The sensing properties of the nanohole chains on glass substrates were compared to short-range ordered nanohole systems fabricated by colloidal lithography on substrates of different refractive index: Teflon ( $n_{Te} = 1.3$ ), glass ( $n_G = 1.5$ ) and  $TiO_2$  ( $n_{Ti} = 2.4$ ). Teflon substrates were obtained by spin coating Teflon resin solution (DuPont) at 5000 rpm for 1 min on a glass slide covered with a Ti adhesion layer. A soft baking at 120 °C for 10 min and at 180 °C for 15 min followed the spin-coating, creating an approximately 600 nm thick Teflon film. Titanium dioxide substrates were fabricated on similar glass slides by reactive sputtering (FHR MS150) with a titanium target and a process gas consisting of a mixture of argon and oxygen. The substrates were patterned with 100 nm diameter holes in 20-nm Au films by colloidal lithography, as follows. The substrates were exposed to oxygen plasma for 10 seconds (Plasmatherm Batchtop m/95) to increase the hydrophilicity of the surface. Subsequently, a polyelectrolyte triple layer was deposited on the samples, creating a positive surface charge for the adhesion of negatively charged sulfate latex spheres [18]. After polyelectrolyte coating, a 0.2% w/v solution of 100 nm diameter spheres (Invitrogen) was dispensed on the samples. Samples were rinsed in DI water and blown dry with nitrogen gas. A metal film consisting of 1 nm of Ti and 19 nm of Au was then evaporated on the samples. Finally, samples were tape-stripped to leave the short-range ordered nanoholes in the thin metal film.

Samples were inspected using an SEM (JEOL JSM-6301F). The spectral characterization of the FIB samples was performed using a fibre-coupled spectrometer (Andor-Shamrock) connected to an inverted dark-field microscope (NikonTE200). Extinction spectra of samples prepared by colloidal lithography were measured using a UV-Vis spectrophotometer (Varian Cary 500).

### 3. Optical sensing of nanohole arrays

To optimize the performance of nanohole systems for bio and chemosensing, it is crucial to know what parameters control their sensitivity. According to Miller and Lazarides [2], the refractive index sensitivity of nanoparticles is increased as the SPR is tuned to NIR. To check if nanohole systems show the same behavior, nanohole chains with different resonant positions were fabricated. The most effective method to tune the resonance of the nanoholes systems is by controlling the separation distance between holes [11]. For this purpose, chains of eight evenly separated nanoholes, 100 nm diameter, in a 20 nm thin Au film were fabricated, Fig. 1 (a). Distances between the holes were varied between 100 and 300 nm. As shown in Fig. 1 (b), the separation distance between holes allows tuning the resonance of the nanohole chain from 650 to 850 nm. On the other hand, Fig. 1 (b) – (d) shows the shift of the peak position when the refractive index of the external media is varied. It is evident that increasing nanohole separation distance and, consequently, tuning the peak position to NIR, results in a larger bulk refractive index sensitivity. However, unlike metal nanoparticles, the increase in the sensitivity is not a linear function of the peak position [2]. This behavior reflects the destructive interaction between nanoholes when their separation distance fits the wavelength of the antisymmetric SPP, i.e., 250-300 nm [11].

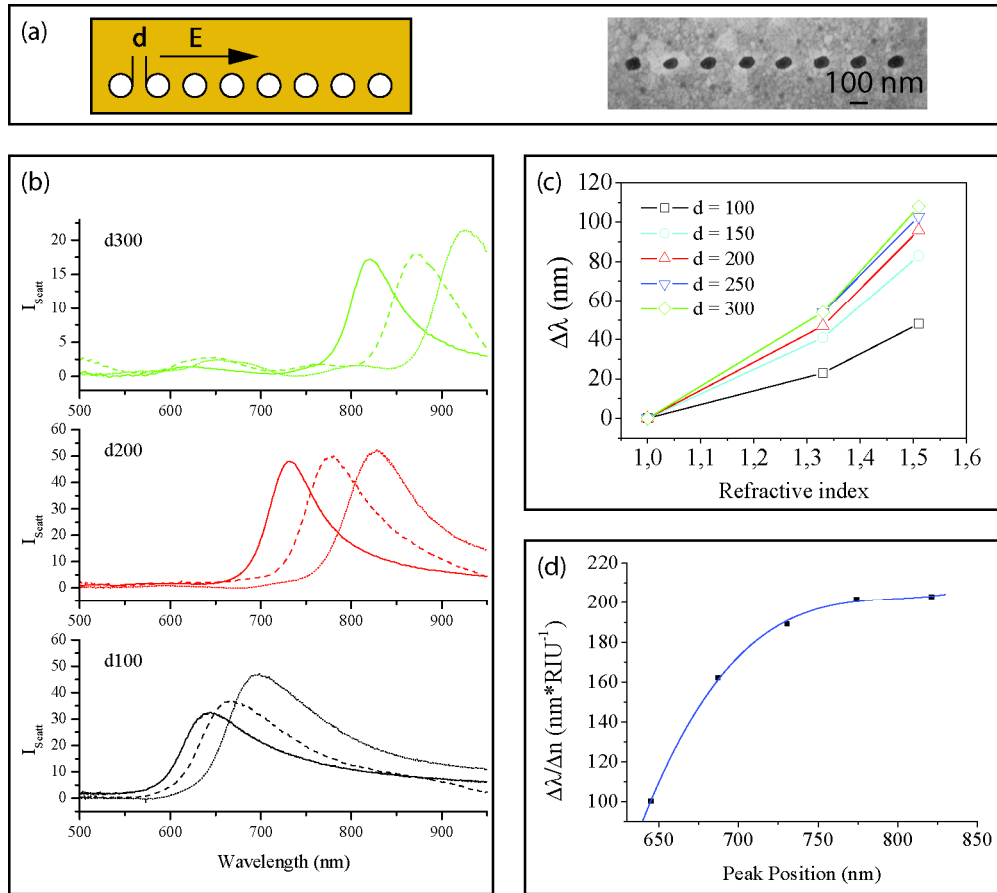


Fig. 1. Nanohole separations enable the tuning of the resonance into the NIR. (a) Illustration and SEM of nanohole chain, indicating polarization and the edge-to edge distance,  $d$ . (b) Scattering spectra for nanohole array with  $d = 300, 200$  and  $100$  nm. The samples are covered with air (solid), water (dashed) and immersion oil (dotted). (c) Difference in peak position as a function of the refractive index of the sensing medium. Separations are given in the legend. (d) Bulk refractive index sensitivity as a function of the spectral peak position. A linear fitting of the data in (c) is used.

In a configuration where the nanoholes are fabricated in metal film on a glass substrate, with an external medium consisting of water or air, the electromagnetic field of the antisymmetric SPP is mainly concentrated in the glass-metal interface (Fig. 2 (a)). As a consequence, the metal film in between nanoholes has a poor sensitivity to the local changes of refractive index, as demonstrated by Dahlin *et al.* [13]. The immobilization of biomolecules inside the nanoholes showed a 16 times stronger response compared to immobilization on Au surface. However, the field distribution of the antisymmetric SPP controlling the interaction between nanoholes can be easily tuned by changing the refractive index of the substrate, as Fig. 2 displays. The reduction of the refractive index pushes the field towards the sensing region (Fig. 2 (b)), while an increase in the refractive index produces a larger concentration of the field in the substrate/metal interface (Fig. 2 (c)). As a consequence of the change in the field distribution, an enhancement of the bulk and surface sensitivities is expected in substrates with low refractive index. In contrast, increasing the refractive index difference between the sensing and substrate regions should reduce the sensitivity.

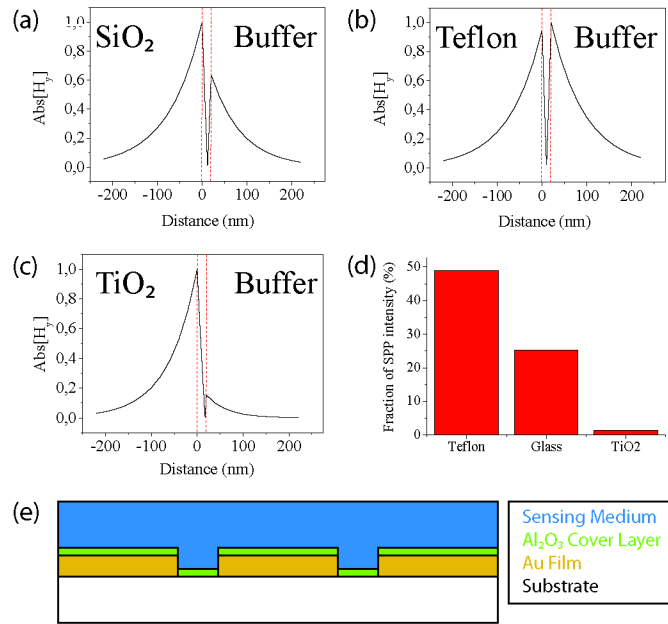


Fig. 2. Calculated field distributions for inhomogeneous gold film environments. (a) Glass (b) Teflon, (c)  $\text{TiO}_2$ . field distributions calculated using the transfer matrix method [19] (d) Fraction of field in sensing within sensing medium (e) Schematic cross-section of a gold film with nanoholes

To test the hypothesis of the substrate influence on the field distribution and sensitivity, we have analyzed the bulk and surface sensitivities in three different substrates: Teflon, glass and  $\text{TiO}_2$ . Since FIB fabrication technique is not suitable for practical applications, we have employed colloidal lithography to pattern gold films with short range ordered nanoholes, keeping the same mean separation distance between nanoholes. Since the mean separation distance between holes in colloidal lithography is governed by the electrostatic interaction between the latex beads and the polyelectrolyte triple layer, the composition of the substrate has a negligible influence on the final distribution of the holes, as Fig. 3 shows. Therefore, all the spectral changes observed in the extinction measurements of the colloidal lithography samples are only due to the change of the substrate's refractive index

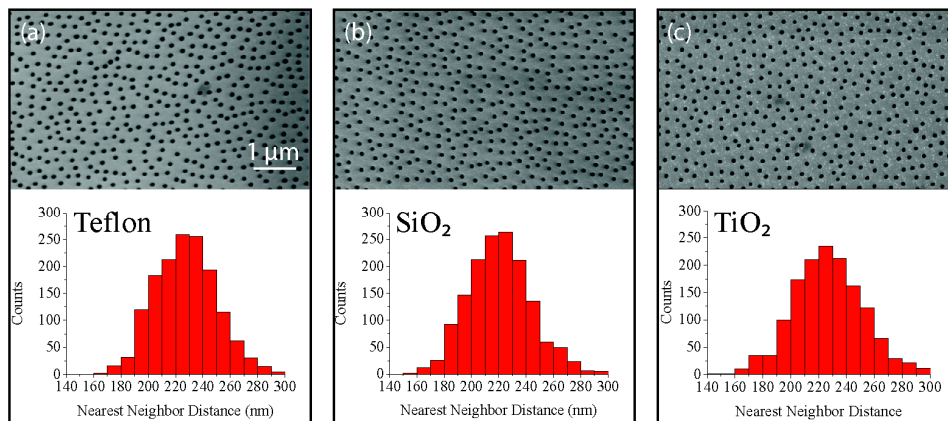


Fig. 3. SEM pictures of nanoholes in gold films prepared by colloidal lithography on different substrates: (a) Teflon (b)  $\text{SiO}_2$  (c)  $\text{TiO}_2$ . Magnification is 16 000x and acceleration voltage is 5 kV. Center-to-center nearest-neighbor distances for the three different substrates are shown.

Spectra of the nanohole arrays in the three substrates are shown in Fig. 4 (a). The first noticeable effect is a blue shift of SPR of the Teflon-coated sample with respect to a bare glass substrate, and a strong red-shift in case of TiO<sub>2</sub>-coated substrate. In the later, the red-shift is accompanied by a substantial broadening due to the increased absorption of antisymmetric SPPs. A stronger absorption induces a great decrease in the propagation distance of SPPs and, consequently, a weaker interaction between holes. It has been observed that the spectra of non-interacting holes are much wider than interacting ones [10, 11].

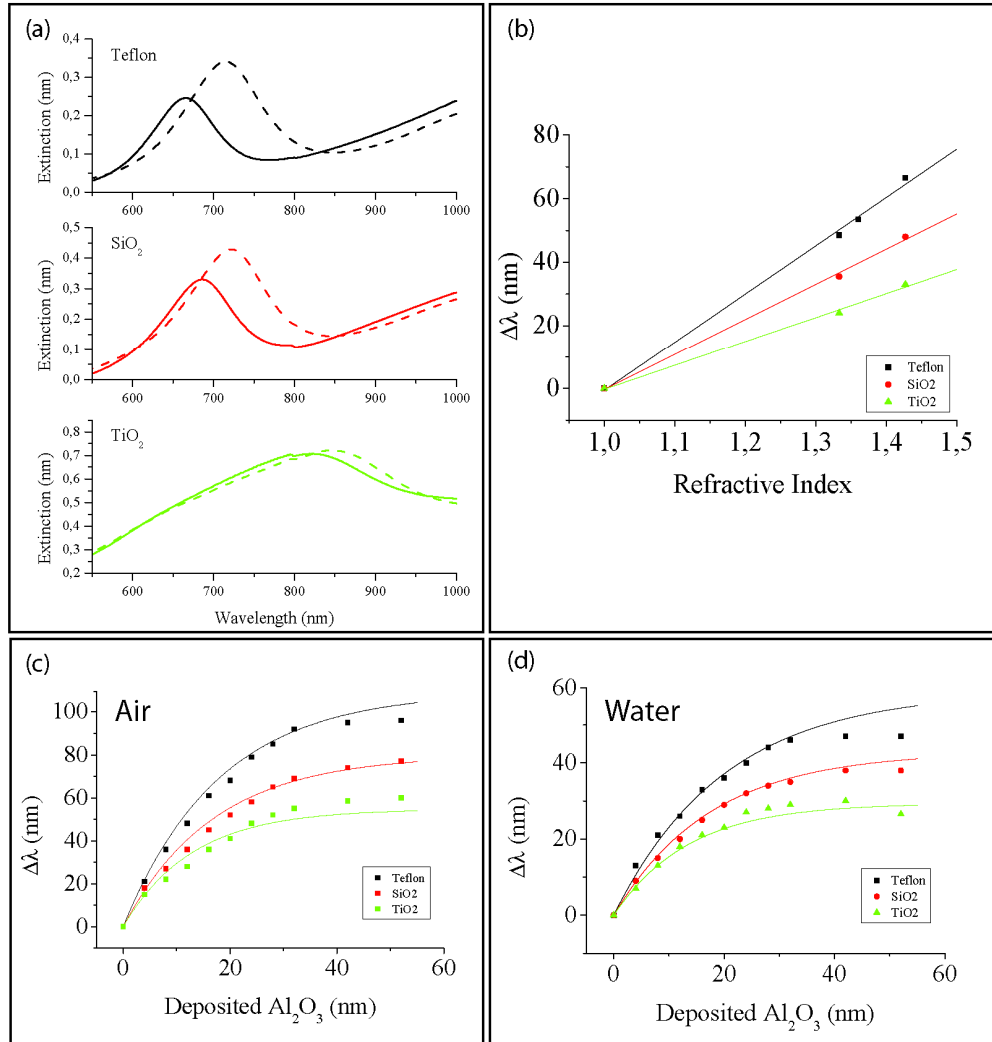


Fig. 4. Extinction spectra for nanohole arrays on Teflon (black), SiO<sub>2</sub> (red) and TiO<sub>2</sub> (green) substrates. (a) Spectral responses due to bulk refractive index changes are shown. Samples are immersed in air (solid) and water (dashed). (b) Bulk refractive index sensitivity. (c) and (d) show measured and fitted surface sensitivities in air and water.

The spectral variations produced by bulk refractive index changes in the sensing medium are shown in Fig. 4 (a) and (b). Interestingly, despite the peak position of the low refractive index substrate is blue-shifted, the sensitivity to the bulk changes of refractive index is enhanced, showing that  $\eta_{bulk}$  is 152, 111 and 76 (RI)<sup>-1</sup>, for Teflon, glass and TiO<sub>2</sub>, respectively.

To model the surface sensitivity due to local changes of refractive index, the peak position as a function of the thickness of  $\text{Al}_2\text{O}_3$  layer, has been measured when the external medium was air and water (Fig. 4 (c) - (d)). Similar to the bulk sensitivity, the surface sensitivity improves as the refractive index of the substrate is reduced, and the improvement factor is approximately equal. These experimental results highlight the importance of the field distribution of the antisymmetric SPP for sensing applications.

Table 1: Experimental values of the bulk and surface sensitivity when the external medium is water, and decay length of the electromagnetic field in the sensing region, extracted from the experimental data.

	Teflon	Glass	TiO <sub>2</sub>
$\eta_{bulk}$ (nm RIU <sup>-1</sup> )	152	111	76
$\eta_{surf}$	3.25	2.25	1.75
$\delta_{air}$ (nm)	36	34	26
$\delta_{water}$ (nm)	40	35	27

#### 4. Discussion

The experimental results show that there are two methods to improve the sensitivity of the nanohole systems: i) increasing the separation distance between holes to red-shift the resonance, and ii) reducing the refractive index of the substrate. Since the peaks are blue-shifted for the Teflon substrate with respect to glass and TiO<sub>2</sub>, the effective improvement of the sensitivity should include the factor induced by the peak position, which can be extracted from Fig. 1 (c). Taking into account such effect, the effective improvement of bulk and surface sensitivities for Teflon is 1.6 and 3 with respect to glass, and TiO<sub>2</sub>, respectively.

In the same way as the rest of nanoplasmonic systems, in nanohole arrays, the decay of the electromagnetic field in the sensing region, so called evanescent field, can be approximately modeled as an exponential decay  $E_i(z)=E_i(0)\exp[-z/\delta]$ , with  $\delta$  being the decay length of the field. With this model, it is possible to get a simple expression for the peak position shift when a dielectric layer is deposited on the sensing interface [20]:

$$\Delta\lambda = \eta_{bulk} (n_f - n_{bulk}) (1 - \exp(-2d / \delta)) \quad (3)$$

where  $n_f$  and  $n_{bulk}$  are the refractive indices of the film and the external medium, respectively. From the best fit of this expression to the experimental data shown in Fig. 4, the penetration depth of the field can be extracted when the external medium is air or water (see Table 1). To get these values, we employ the experimental bulk sensitivities and a refractive index of 1.72 for the  $\text{Al}_2\text{O}_3$  layer. This simple model is not valid for thickness above 30-35 nm, as shown by Rindzevicius *et al.*[21], due to an image dipole effect caused by the dielectric film. The result of such effect is a faster decay of the peak red-shift for dielectric films thicker than 35 nm, and oscillatory behavior of the peak position for even thicker dielectric films [21].

The comparison of our measured decay lengths for the SiO<sub>2</sub> substrate with the simulations of Rindzevicius *et al.* [9], rendering a 40 nm decay length for 107 nm sized holes on a SiO<sub>2</sub> substrate, confirms the applicability of the model. These values show that the penetration of the field is larger for Teflon substrates, especially when water is the external medium. In this case, the maximum amplitude of the electromagnetic field of SPP is in the metal/external medium interface, as Fig. 2 (b) displays. The observed increase in the surface and bulk refractive index sensitivity can be mainly assigned to a greater penetration depth of the surface plasmon polariton into the sensing region. The larger penetration could explain as well the non-linear bulk refractive index response seen in Fig. 1 (b) and Fig. 4 (b). In the previous work by Dahlin *et al.*, the sensitivity of the metal region was much smaller than the holes when the substrate is glass. Since the fraction of the field of the antisymmetric SPP in the sensing region is larger for Teflon than glass, corresponding approximately to the effective increase in sensitivity, the metal film on Teflon substrates is more sensitive. In contrast, in the case of TiO<sub>2</sub> the amount of SPP field in the sensing region is so small, that the sensitivity of the metal region will be negligible and the sensing response will come principally from the



nanoholes. Employing substrates with lower refractive index than Teflon, such as porous silica, it could possibly have further improvements on the sensitivity.

## **5. Conclusions**

We have shown in this work that substrate modification allows a way of controlling the electromagnetic near-field distribution of the nanohole arrays. Minimizing the substrate refractive index enhances the sensitivity of nanohole arrays as the field is directed into the sensing region. Even though this modification induces a blue-shift of the resonance position, the sensing response to bulk and local refractive index changes is increased. The sensitivity improvement can be mainly assigned to an increase of the sensitivity in the metal region between holes. The combination of optimized sensitivity together with the chemical contrast in the nanohole arrays, make this sensing platform very attractive for biosensing applications. This method to tailor the field distribution can also find important nanophotonic applications.

## **Acknowledgments**

We thank Dr. Tavakol Pakizeh for fruitful discussions. B. Brian and M. Käll acknowledge the financial support from Swedish Research Council and Swedish Foundation for Strategic Research. B. Sepulveda and L. M. Lechuga acknowledge the financial support from M. Botin Foundation.